Chapter 3
Evolutionary Algorithms Based on Structured Coding for Aerodynamic Wing Optimizations

3.1 Introduction

The difficulty in finding the global optimum in an aerodynamic shape design optimization problem stems in a large part from its high degree of nonlinearity in the objective function distribution. When EAs are used to solve engineering optimization problems, the term *epistasis* is often used to describe nonlinearity in the objective function distribution [1]. In highly epistatic problems, many of the design parameters strongly interact with each other and thus, it is very difficult to decompose such design problem into independent subproblems. Since EAs typically optimize by combining valid features (sets of dependent parameters) of different design candidates, the robustness and efficiency of EAs decrease significantly for such design problems. Therefore, if the epistatic interaction structures of the design parameters are identified in advance, the robustness and efficiency of EAs can work more robustly and efficiently by rearranging encoding of the design parameters.

To illustrate this, consider two sequentially coded design candidates (Parent1&2) where there are strong interactions between real design variables **a** and **e** as well as **b** and **d** (Fig. 3.1).

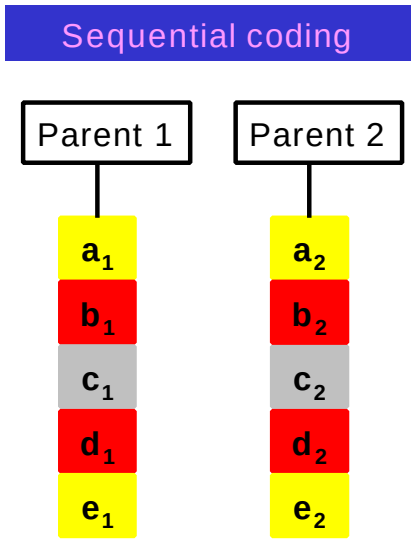

Fig. 3.1 Sequentially coded design candidates

Application of one-point crossover at any site would wind up destroying the above combinations. In such a case EAs would not work well. Consider now an alternative arrangement, in which interactive design parameters are grouped as Fig. 3.2.

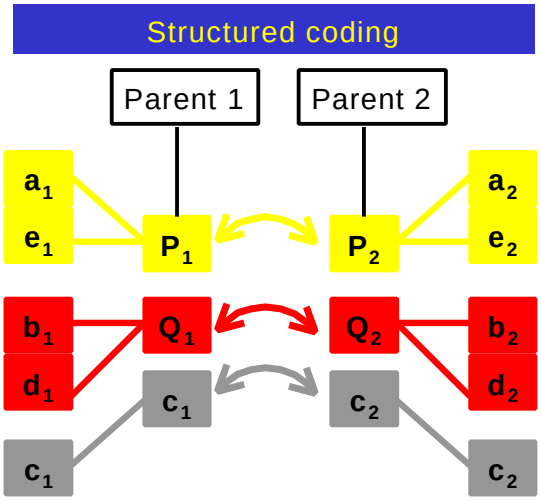

Fig. 3.2 Design candidates coded with structure

In this case, no matter whether one-point crossover is applied to between **P** and **Q** or between **Q** and **c**, the combinations of the dependent design parameters are preserved.

For analysis of concerning design problems, a parametric study is often conducted by varying one parameter at a time or by trial and error for a limited number of parameters. However, such approaches only lead to incomplete knowledge for a large design space. An exhaustive search, in contrast, requires unacceptably large number of experiments and thus they are not suitable to real-world problems. For instance, a full factorial design of a design space of 10 parameters with 3 levels would require $3^{10} = 59049$ experiments. The use of such a time consuming approach is prohibitive for the preprocessing epistasis analysis.

An efficient approach is *experimental design* that can gain required information at the least expenditure of resources. The underlying idea of this statistical technique is that the number of experiments can be reduced by extracting the required information, often the main effects and 2-factor interactions, assuming that higher order of interactions are negligible in typical design problems. This technique construct algebraic approximations of the objective function distribution with a set of experiments carefully distributed throughout the design space using so-called orthogonal array and then, the effectiveness of the factors and their interactions are estimated by F-tests (for more detail, see [2])

The objective of this chapter is to improve robustness as well as efficiency of EAs by introducing the structured coding based on the epistasis analysis. Experimental design will be used to examine the epistatic interaction structures of design parameters. First, feasibility of typical airfoil shape parameterization techniques will be examined though reproduction of a NASA supercritical airfoil and an aerodynamic airfoil shape optimization in Sec. 3.2. Then, the present approach will be applied to aerodynamic design of a wing shape in Sec 3.3.

3.2 Comparative Study of Airfoil Shape Parameterization Techniques

In recent years, the development of automated design process for aerodynamic design is actively studied by many researchers. For instance, more than twenty papers related to aerodynamic or multidisciplinary optimization by numerical methods were presented in the 38th AIAA aerospace sciences meeting and exhibit held on January 2000. In spite of such vigorous investigations, as is the case in any new research field, many questions remain unanswered. Parameterization of the design space, as well as choice of optimization methods, is one of the most outstanding issues of concern.

There are three objectives in developing a parameterization technique:

1) A parameterization technique should have adequate flexibility. Otherwise, the global optimum design may be excluded from the design space. For example, if a transonic airfoil shape were designed using NACA four-digit airfoils, the obtained airfoil would have high wave drag under a

certain thickness constraint.

2) The number of required parameters should be kept as low as possible since it corresponds to the number of dimensions of a design space. An extreme example is reported in [3] where a three-dimensional wing shape was parameterized by using the location of each surface mesh point as design parameters. This approach required more than 4000 design parameters. The final result was therefore subject to constraints and the additional geometry smoothing. It is not efficient to find a global optimum design in such a large design space.
3) Design parameters should control important features of the given design problem. Because such parameters are likely to be independent of each other, optimization can be conducted efficiently. One may recall that early studies on airfoil properties in subsonic flow were efficiently demonstrated by dividing an airfoil shape into thickness distribution and camber line. On the other hand, a design parameter set that is chosen without knowledge of the given design problem would have complex interaction among them providing a complex objective function landscape. Finding a global optimum is very difficult in such an optimization problem.

Although many researchers have proposed airfoil shape parameterization techniques to achieve their goals, there is no comparative study of airfoil shape parameterization techniques aside from a work of Reuther and Jameson [4] within the author's knowledge. In this section, some typical airfoil parameterization techniques will be compared to clarify this open issue.

3.2.1 Airfoil Shape Parameterization Techniques

3.2.1.1 Extended Joukowski Transformation

Equation (3.1) is well known as the Joukowski transformation that transforms a circle into various airfoils:

$$V = z + \frac{1}{z} \tag{3.1}$$

The extended Joukowski transformation [5] gives further variety in the resultant airfoil shapes using a preliminary transformation before the Joukowski transformation as:

$$z' = z - \frac{e}{(z - \Delta)} \tag{3.2}$$

$$V = z' + \frac{1}{z'} \tag{3.3}$$

where e and D are a complex number and a real number, respectively. The airfoil shape is defined by 5 parameters: center of the circle Z_c, real part and imaginary part of e, and D. An example of the extended Joukowski transformation is illustrated in Fig. 3.3.

Instead of the raw design variables (Z_c, e, D), the present design variables are given by (x_c, y_c, x_t, y_t, D) where the center of the circle Z_c and the complex number e correspond to the position (x_c, y_c) and (x_t, y_t), respectively. D is the preliminary movement in the real axis. It is known that x_c and x_t are related to the airfoil thickness while y_c and y_t are related to the airfoil camber.

3.2.1.2 Inverse Theodorsen Transformation

Any given airfoil shape can be transformed into a unit circle using the Theodorsen transformation [6] that consists of the following Joukowski transformation and the primary approximation:

$$V = z' + \frac{1}{z'} \tag{3.4}$$

$$z' = z \exp\left(\sum_{0}^{\infty} \frac{C_n}{z^n}\right) \tag{3.5}$$

where the complex numbers C_n are determined by the fast Fourier transformation. The inverse of the Theodorsen transformation can be used to parameterize an airfoil shape. The accuracy of this technique depends on the truncation of summation in Eq. (3.5). In this study, an airfoil shape is defined by 13 parameters, which corresponds to the truncation at the sixth term.

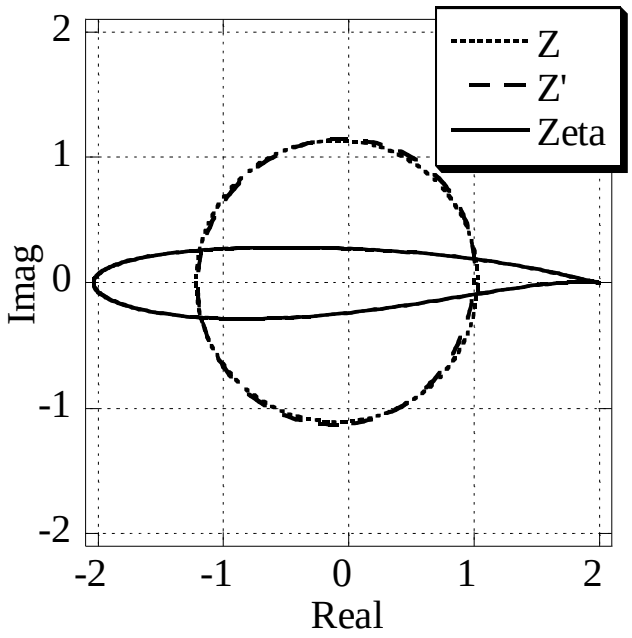

Fig. 3.3 Example of the extended Joukowski transformation

3.2.1.3 B-Spline Curves

Parameterization using the third-order B-Spline curves is one of the most popular approaches for airfoil designs (for example, see [7,8]). The design parameters are positions of control points of the B-Spline curves. In this study, an airfoil shape is split into a mean camber line and thickness distribution. Five control points are used for each of the mean camber line and the thickness distribution (Fig. 3.4). Since locations of the leading edge and trailing edge are frozen, 12 design variables are required to give an airfoil shape.

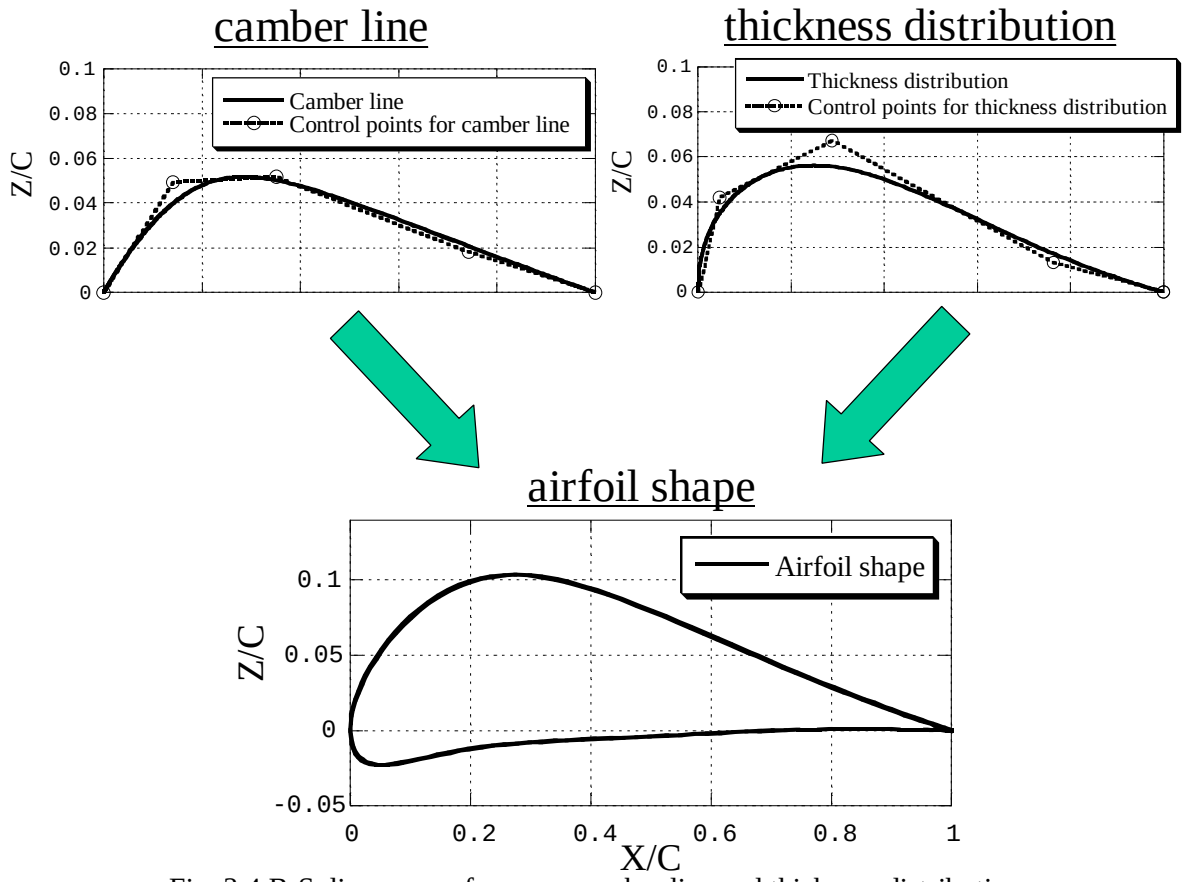

Fig. 3.4 B-Spline curves for mean camber line and thickness distribution and the resultant airfoil shape

3.2.1.4 Orthogonal Shape Functions

There is a class of parameterization techniques based on linear combination of shape functions. In Ref. 9, Chang *et al*. have proposed a polynomial function to parameterize upper and lower surfaces of an airfoil using orthogonal shape functions to reduce the required design parameters:

$$Z = a_1(x^{\frac{1}{2}} - x) + \sum_{n=2}^{6} a_n(x^{n-1} - x^n) + \sum_{n=7}^{10} a_n(x^{\frac{1}{n-4}} - x^{\frac{1}{n-5}}) \qquad (3.6)$$

This approach for the airfoil parameterization is a derivative of the original NACA method [10]. The number of parameters is 20.

3.2.1.5 PARSEC Airfoils

An airfoil family “PARSEC” has been recently proposed to parameterize an airfoil shape [11]. A remarkable point is that this technique has been developed aiming to control important aerodynamic features effectively by selecting the design parameters based on the knowledge of transonic flows around an airfoil.

Similar to 4-digit NACA series airfoils, The PARSEC parameterizes upper and lower airfoil surfaces using polynomials in coordinates *X*, *Z* as,

$$Z = \sum_{n=1}^{6} a_n \cdot X^{n-1/2} \qquad (3.7)$$

where a_n are real coefficients. Instead of taking these coefficients as design parameters, the PARSEC airfoils are defined by basic geometric parameters: leading-edge radius, upper and lower crest location including curvatures, trailing-edge ordinate, thickness, direction and wedge angle as shown in Fig. 3.5. These parameters can be expressed by the original coefficients a_n by solving simple simultaneous

equations. Eleven design parameters are required for the PARSEC airfoils to define an airfoil shape in total. For comparison purpose, both the trailing-edge thickness and its ordinate (at X=1) were frozen to 0. Therefore, nine design variables are used to give an airfoil shape in the following sections.

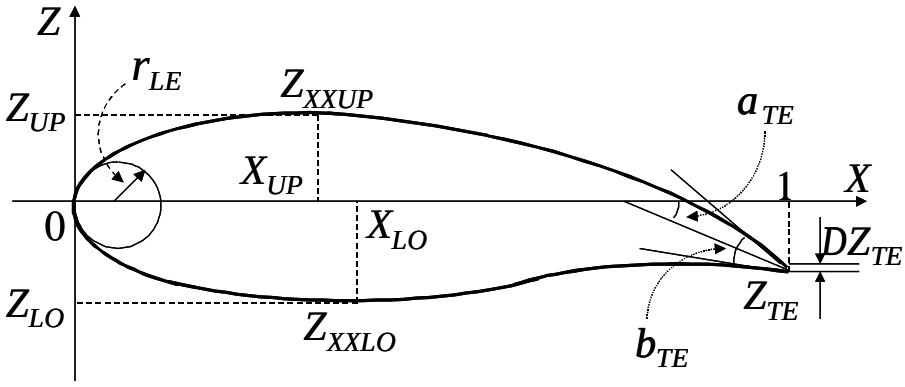

Fig. 3.5 Design parameters for the PARSEC

3.2.2 Reproduction of a NASA Supercritical Airfoil

To examine flexibility of the above parameterization techniques, reproduction of a NASA supercritical airfoil SC(2)-0414 was demonstrated by minimizing differences between the SC(2)-0414 airfoil geometry and airfoil shapes reproduced by the parameterizations (see Fig. 3.6). A real-coded Adaptive Range Genetic Algorithm (ARGA, see Chap.2) was used for minimization. In the evolutionary process, 300 generations are run for five times with a population size of 200.

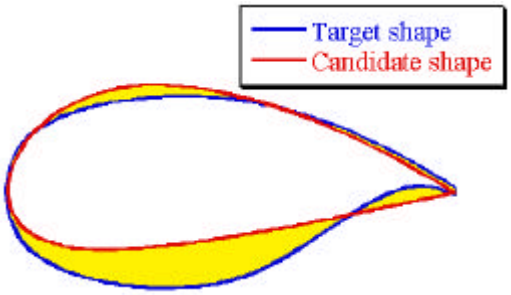

Fig. 3.6 Area to be minimized

The reproduced airfoils and the corresponding residuals are presented in Figs. 3.7 and 3.8, respectively. It should be noted that five runs were performed for each airfoil but the difference was negligible. The results show that the SC(2)-0414 airfoil is included in the parameterized space of PARSEC, Theodorsen, and B-Spline airfoils. The residuals of those airfoils in Fig. 3.8 are not converged to machine-zero due to the brunt trailing edge of the SC(2)-0414 airfoil. On the other hand, the extended Joukowski airfoil and the airfoil using orthogonal shape functions have failed to reach the SC(2)-0414 airfoil. The failure of the extended Joukowski airfoil results from its insufficient design space. To find the cause of the failure of the orthogonal shape functions, reproduction of NACA 2412 airfoil was performed. Figure 3.9 shows the target airfoil shape and the most approximate shape with five trials obtained by the EA using the orthogonal shape functions. Although the set of the orthogonal shape functions includes the generator of the NACA 4-digit airfoils, the present EA has failed to reach the NACA 2412 airfoil. These results indicate that the parameterization using orthogonal shape functions is not suited for EA-based optimization.

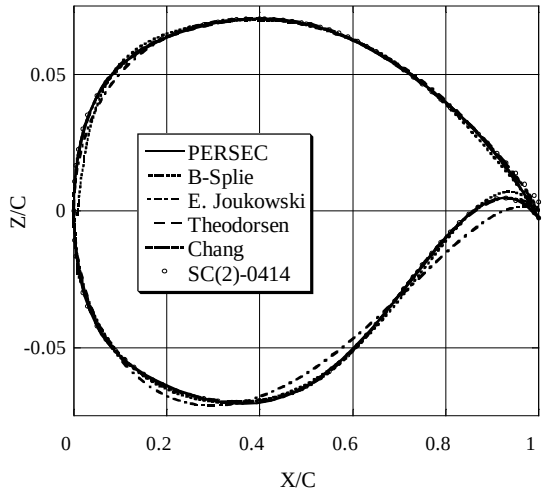

Fig. 3.7 Comparison of the reproduced airfoils

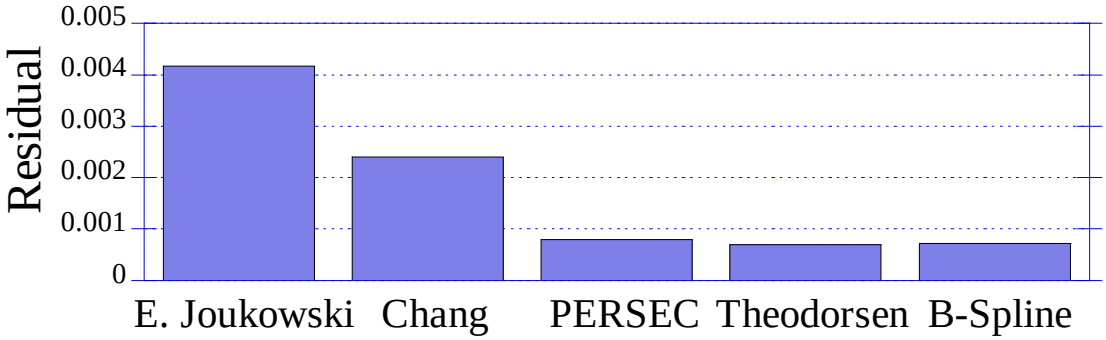

Fig. 3.8 Residual of the SC(2)-0414 airfoil reproduction

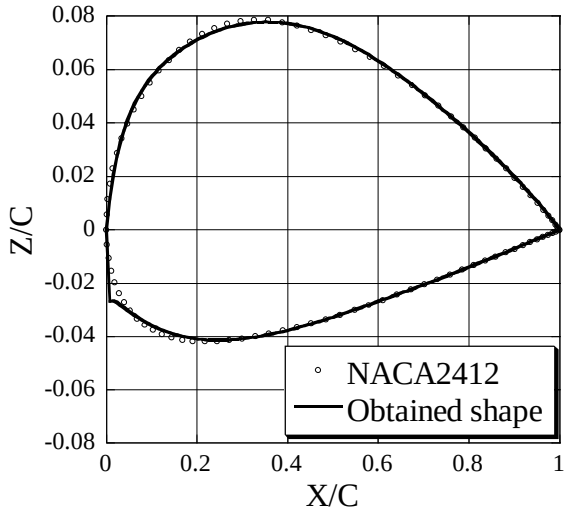

Fig. 3.9 NACA 2412 and the airfoil shape obtained by orthogonal shape functions

3.2.3 Aerodynamic Shape Optimization

Aerodynamic airfoil shape optimizations were demonstrated to examine the search efficiency of the parameterization techniques further. The objective function was the lift-to-drag ratio L/D to be

maximized. The free stream Mach number and the angle of attack were set to 0.8 and 2 degrees, respectively. The aerodynamic performance of each design was evaluated by the two-dimensional Navier-Stokes solver described in Chap.4. The airfoil thickness was constrained so that the maximum thickness was greater than 12% of the chord length. The real-coded ARGA was used to maximize the objective function where the population size and the number of generations were both 100. Because EAs are stochastic optimization algorithms, two trials were performed for each airfoil parameterization.

Figure 3.10 shows the optimization histories. The aerodynamic performances of the design results are summarized in Table 3.1. These results ensure that the performance of the designed airfoil greatly depends on the choice of the parameterization techniques.

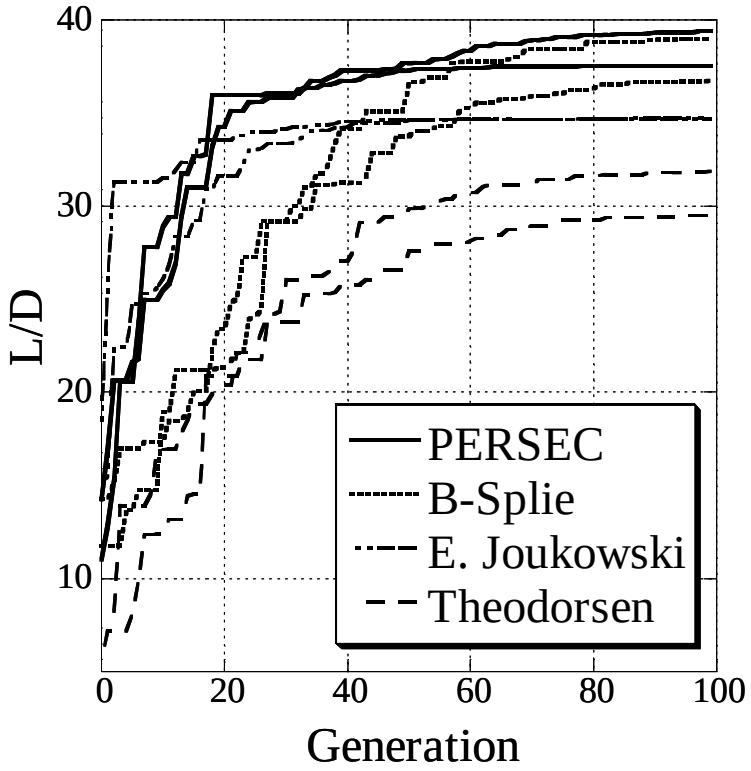

Fig. 3.10 Optimization histories

Table 3.1 Results of aerodynamic optimizations

	Theodorsen	Extended Joukowski	B-Spline	PARSEC
L/D	31.87	34.73	39.02	39.40
C_l	0.5535	0.5427	0.6223	0.6253
C_{od}	0.01737	0.01562	0.01595	0.01587

The present EA using the PARSEC airfoils has reached to the airfoil shape of the best performance. Because the parameter set of the PARSEC airfoils represents aerodynamically important features of an airfoil shape in transonic regime, they are to some extent independent and thus, the present EA could search the design space efficiently. This parameterization gives the design space wide enough as shown in the previous section, which also helps finding a global optimum.

The resulting airfoil shape and the corresponding Cp distribution are shown in Fig. 3.11. The surface pressure distribution is similar to that of NASA supercritical airfoils, such as an approximately uniform distribution (rooftop) on the upper surface, a weak shock wave significantly aft of the midchord, a pressure plateau downstream of the shock wave, a relatively steep pressure recovery on the extreme rearward region, and a trailing edge pressure slightly more positive than ambient pressure [12]. The design result is considered to be the global optimal and thus ensures the feasibility of the present approach.

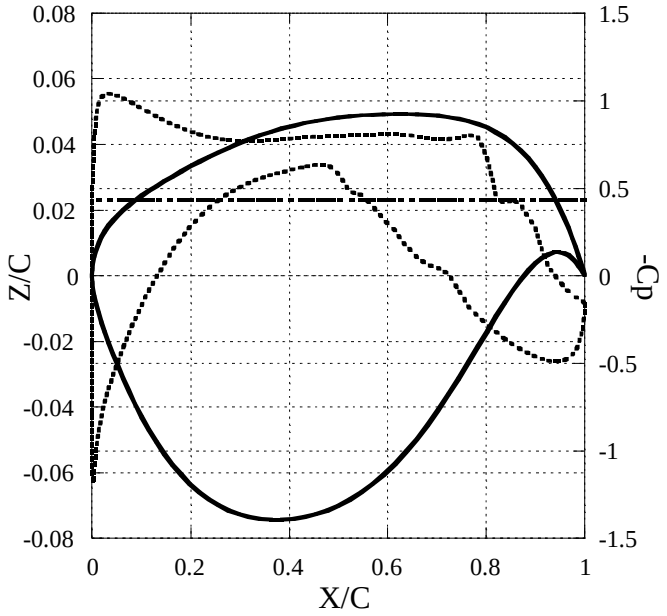

Fig. 3.11 Designed airfoil shape and the corresponding pressure distribution using PARSEC airfoils

EA using the B-Spline curves has succeeded in finding a reasonably good airfoil design but the performance of the resulting airfoil is slightly less than that optimized by the PARSEC airfoils. The reason is probably the selection of the design parameters. The locations of B-Spline control points are not related to the flow physics in contrast to the parameter set of the PARSEC airfoils.

The resulting airfoil obtained from the inverse Theodorsen transformation performed worst. To check whether the design obtained by the PARSEC airfoils is included in the search space of the inverse Theodorsen transformation, airfoil reproduction was tried as shown in Fig. 3.12. While the extended Joukowski airfoil has failed to express the best design, the others including the inverse Theodorsen transformation have succeeded. This indicates that the worst performance of EA using the inverse Theodorsen transformation is not due to its insufficient search space but the complex objective function distribution. Because the parameters of the inverse Theodorsen transformation are not defined based on the flow physics around an airfoil, they are likely to have complex interaction of each other. Because EAs typically optimize by combining valid features (sets of dependent parameters) of different design candidates, the robustness and efficiency of EAs decrease significantly for such design problems.

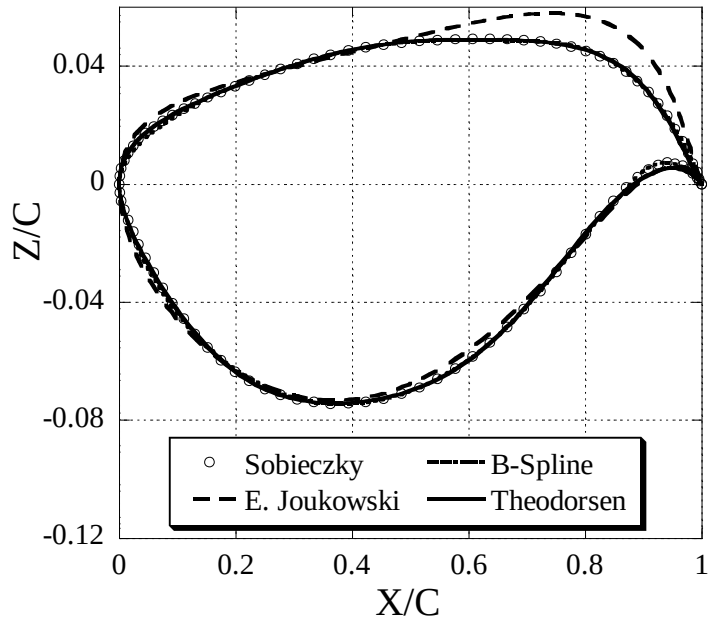

Fig. 3.12 Reproduction of the airfoil design obtained by PARSEC airfoils

The extended Joukowski transformation has found an airfoil that performs better than the inverse Theodorsen transformation. This is due to a relatively small number of design parameters and thus a smaller search space. The other reason is that (x_c,x_t) and (y_c,y_t) are related to the airfoil thickness and the mean camber line, respectively. They are important factors for airfoil performance. As shown in Fig. 3.12, however, the design space is too small to obtain a global optimum for the airfoil design.

3.3 Wing Design Using EAs Based on Structured Coding

3.3.1 Formulation of Optimization Problem

The present design problem is an aerodynamic optimization of a transonic wing shape at the transonic cruise design point. The cruising Mach number is assumed to be 0.8. The objectives functions of the design problem are lift coefficient C_L to be maximized and drag coefficient C_D to be minimized. Therefore, the purpose of the present optimization is to find tradeoff solutions between maximization of C_L and minimization of C_D within one optimization. Airfoil thickness is constrained so that the maximum thickness is greater than 0.08 of the chord length.

The aerodynamic performances are evaluated by using FLO-27, which is the conservative full-potential code developed by Jameson and Caughey [13]. FLO-27 can solve flow around a wing very rapidly: within a few seconds on a vector computer.

The wing planform is that for a typical transonic aircraft as [14] (Fig. 3.13). The extended Joukowski transformation or the PARSEC is used for wing profile parameterization. Airfoil sections defined by these parameters and the twist angle will be given at five spanwise sections. The wing surface is linearly interpolated between the specified spanwise sections. The numbers of the required design parameters are 30 for the wing parameterized by the extended Joukowski transformation and 55 for the wing parameterized by the PARSEC.

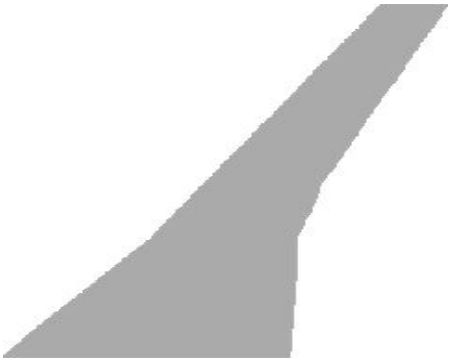

Fig. 3.13 Wing planform

3.3.2 Optimization Using MOEA

In the following calculations, a real-coded MOEA is used for optimization. In the present MOEA, random parental selection and best-*N* selection based on Pareto-ranking method coupled with fitness sharing are used. Since the strong elitism is used, high mutation rate of 0.2 is applied and a random disturbance is added to the parameter in the amount up to±20% of the design space. Population size and maximum number of generations are set to 64 and 300, respectively. Unbiased initial population is generated by randomly spreading solutions over the entire design space in consideration.

3.3.3 Wing Design Using Extended Joukowski Transformation

3.3.3.1 Construction of Structured Coding

Prior to the design optimization, experimental design is applied to analyze the epistatic interaction structures of the design variables. Analysis of interactions of all design variables for the wing model, however, requires unacceptably large number of CFD runs even with the experimental design. Therefore, the design variables are grouped into spanwise variations of the airfoil shape parameters and the twist angle. Factors examined are these spanwise distributions and their two-factor interactions except for those related to the twist angle a. Three types of spanwise variations are considered as levels: no variation, linear increase from root to tip, and vice versa. Examined responses are C_L and C_D of the wing. Only to account for positive responses in aerodynamic performance (increase in C_L and decrease in C_D), following two functions are introduced:

$$F1 = \max (C_L - C_{L0} , 0) \tag{3.8}$$

$$F2 = - \min (C_D - C_{D0} , 0) \tag{3.9}$$

where C_{L0} and C_{D0} are those of a wing having a constant airfoil section along the spanwise direction.

Since this is the case of six factors, ten interactions, and three levels, 81 CFD runs are conducted according to the L_{81} (3^{40}) orthogonal array. Then the results are statistically analyzed by F-tests. Figure 3.14 shows the F values of the examined factors and interactions. The solid and broken lines are critical F values with 1% and 5% statistical risks, respectively. A factor or an interaction that has F value more than these critical values is judged effective. While every single factor is effective on both F1 and F2, nothing but $x_c x_t$ and $y_c y_t$ appears effective among the examined interactions. This result is consistent with the fact that x_c and x_t, are related to the airfoil thickness while y_c and y_t are related to the airfoil camber line.

To make use of identified interaction structures of the design variables,

1) Structured coding is introduced by considering each spanwise distribution of the airfoil parameters and the twist angle as a string of design variables instead of conventional sequential coding where all design variables are coded as a single string.
2) One-point crossover is applied to each string where the same gene site is selected for each interactive design parameter sets (x_c,x_t) and (y_c,y_t), at the probability:

$$\boldsymbol{prob} = 0.1 + 0.7(\min(1, \boldsymbol{generation} / 50)) \qquad (3.10)$$

Figure 3.15 illustrates the proposed structured coding for the present wing shape modeling. The broken lines in the figure show how one-point crossover is applied to the present structured coding. This crossover enables that the genes of the identified parameter sets, such as (x_c x_t) and (y_c y_t) are exchanged together to utilize efficiently the effects of the interactions between them.

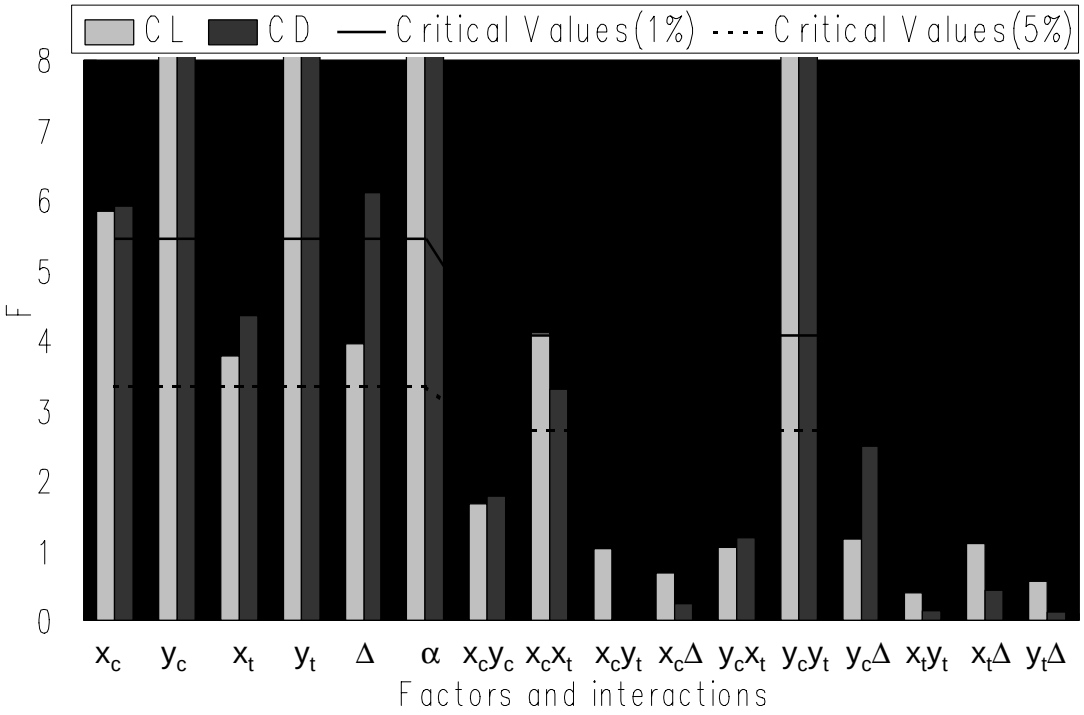

Fig. 3.14 Effectiveness of factors and their interactions for the extended Joukowski transformation

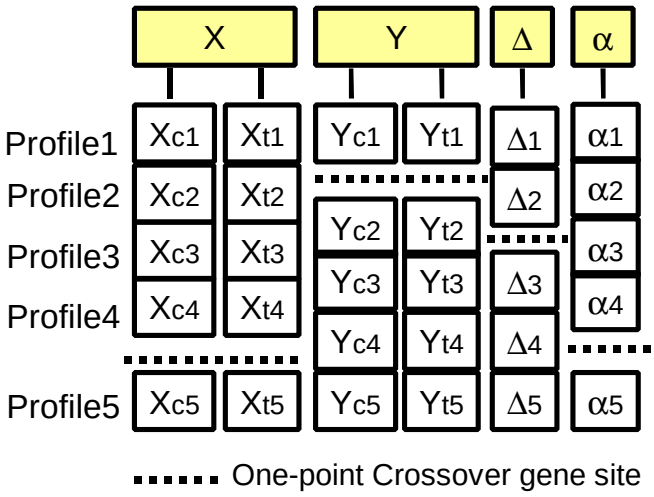

Fig. 3.15 Structured coding for the extended Joukowski transformation

3.3.3.2 Design Results

To validate advantage of the crossover with the structured coding, design optimization is demonstrated. The design results obtained by the present approach are compared with that of the EA with the sequential coding where one-point crossover is applied to each spanwise distribution of the design parameters but each crossover gene site is selected independently as illustrated in Fig. 3.16. Figure 3.17 shows the Pareto optimal solutions indicating the tradeoff between maximization of C_L and minimization of C_D. Solid and hollow points show the resulting Pareto fronts obtained from the sequential and structured codings, respectively. This figure indicates that the present EA with the structured coding had better Pareto solutions in high C_L region.

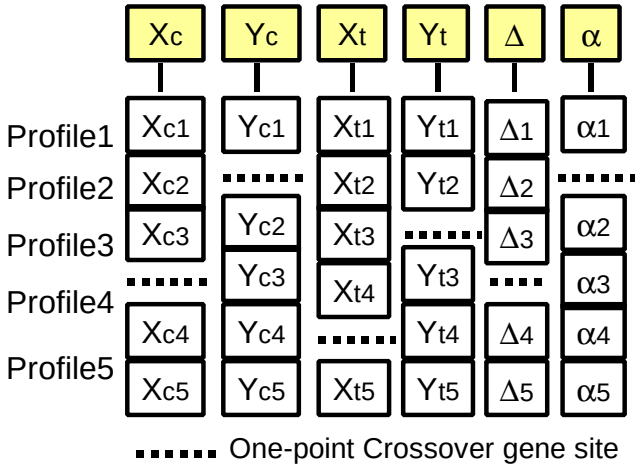

Fig. 3.16 Sequential coding for the extended Joukowski transformation

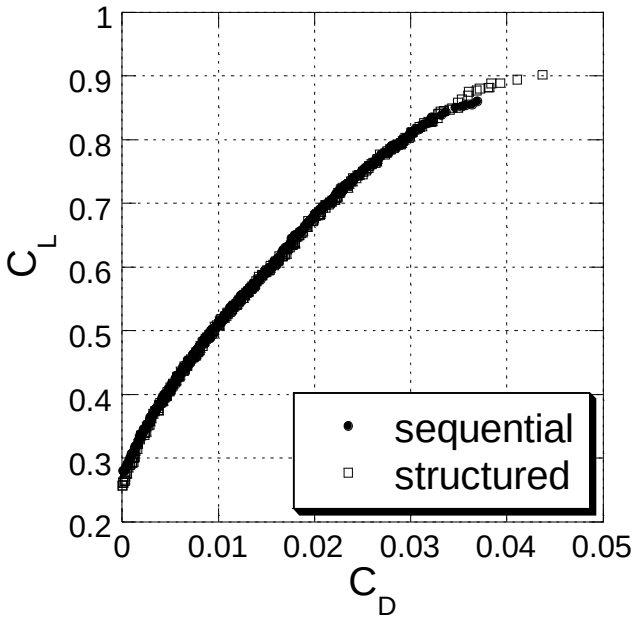

Fig. 3.17 Comparison of Pareto fronts for sequential and structured coding techniques

3.3.4 Wing Design Using PARSEC Airfoils

3.3.4.1 Construction of Structured Coding

Now, the present approach is applied to wing design using the PARSEC. First, the interaction structures of the parameter sets for the PARSEC airfoils are analyzed by the experimental design. The factors to be examined are r_{LE}, X_{UP}, Z_{UP}, Z_{XXUP}, X_{LO}, Z_{LO}, Z_{XXLO}, α_{TE}, Z_{TE} and their two-factor interactions on F1 and F2. The wedge angle at the trailing edge and its interactions are neglected since the wedge angle is primary determined by the structural strength. Also, interactions of $r_{LE}Z_{TE}$, $r_{LE}\alpha_{TE}$ and $r_{LE}Z_{XXLO}$ are disregarded. Consequently, 42 factors are examined by the experimental design

conducted according to the $L_{729}(3^{364})$ design template. Number of CFD runs required for this epistasis analysis is reduced from $3^9 = 19683$ (full factorial design) to $3^6 = 729$.

Figure 3.18 shows the result of the F-tests. Interactions effective in both C_L and C_D are illustrated with bold lines in Fig. 3.19. Since these figures indicate complicated interactions among the design variables, especially, Z_{UP}, Z_{LO}, and Z_{TE}, it seems difficult to construct a structured coding for these design variables. Therefore, new parameters Z_C and Z_H are introduced instead of Z_{UP} and Z_{LO} as:

$$Z_C = (Z_{UP} + Z_{LO}) / 2 \quad (3.11)$$

$$Z_H = (Z_{UP} - Z_{LO}) \quad (3.12)$$

where Z_C and Z_H correspond to airfoil camber and thickness, respectively. Using these parameters, interactions are greatly simplified as shown in Fig. 3.20. According to this result, a structured coding for the spanwise distributions of airfoil parameters is introduced.

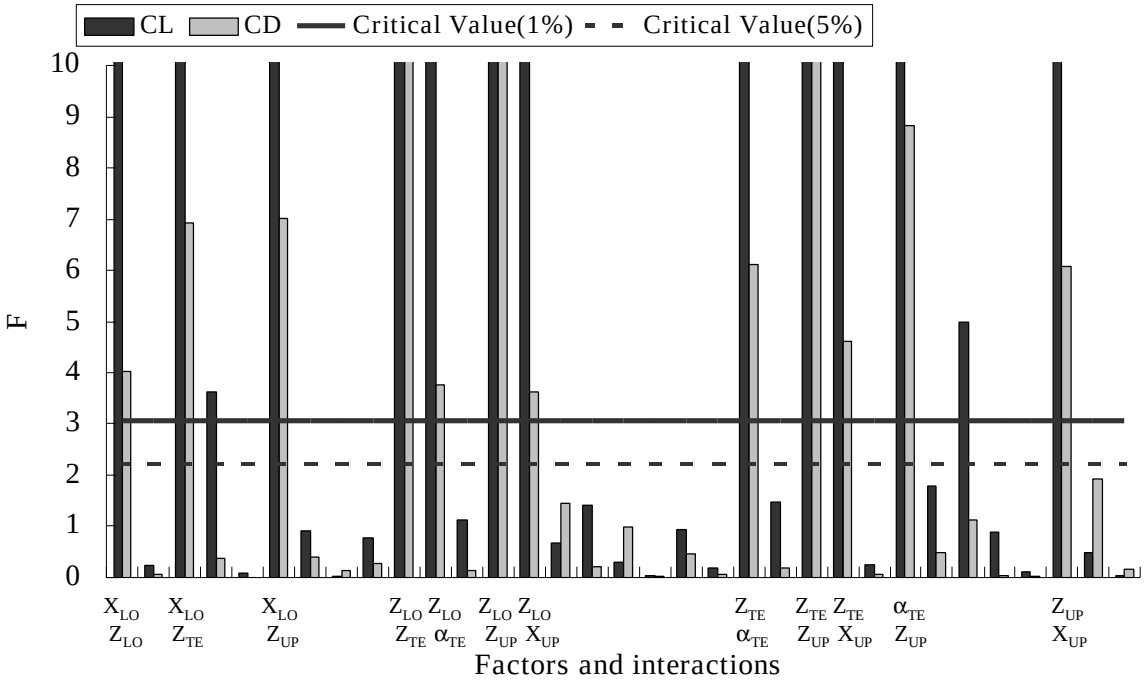

Fig. 3.18 Effectiveness of factors and their interactions for the PARSEC

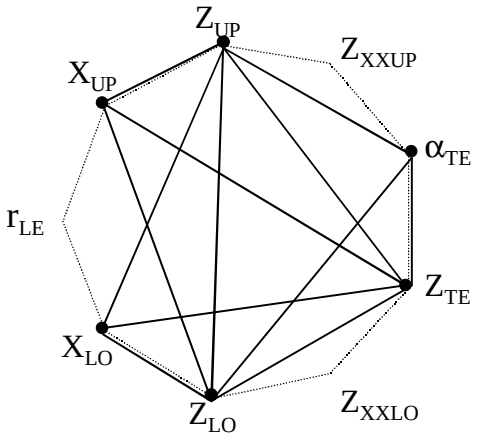

Fig. 3.19 Effective interactions of the original PARSEC

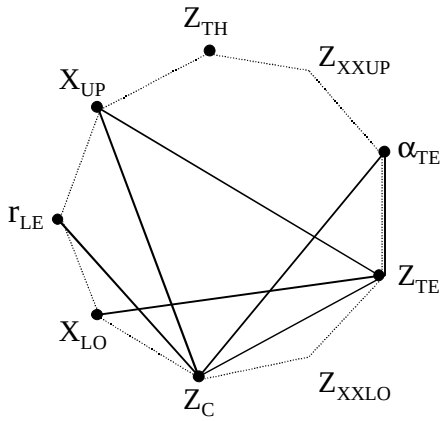

Fig. 3.20 Effective interactions of the modified PARSEC

3.3.4.2 Design Results

The design result obtained by the EA using the crossover based on the structured coding is compared with that obtained by the EA using the sequential coding. Figure 3.21 compares Pareto fronts obtained from the sequential coding of the original PARSEC airfoils and the structured coding using Z_C and Z_H. Similar to the previous section using the extended Joukowski airfoils, advantage of the crossover based on the structured coding is observed in high C_L region. Compared with Fig. 3.17, this figure also illustrated that Pareto front of the PARSEC airfoils is superior to that of the extended Joukowski airfoils.

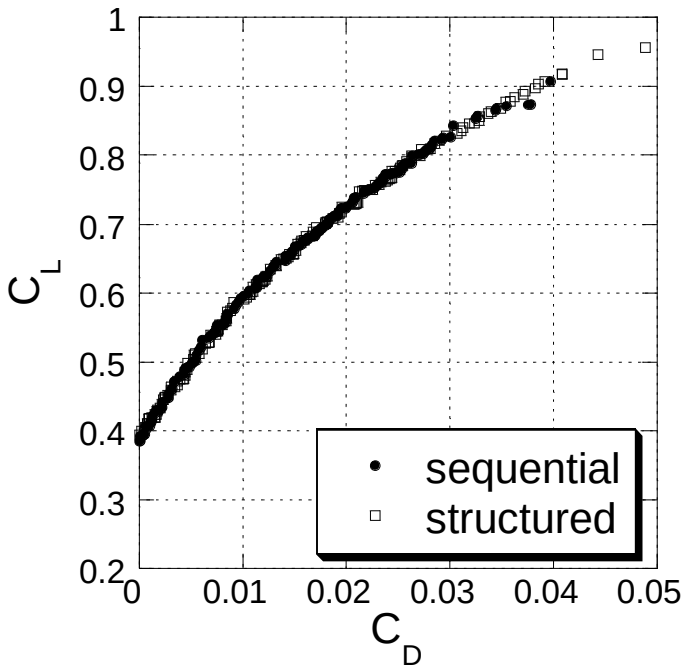

Fig. 3.21 Comparison of Pareto fronts for sequential and structured coding techniques

3.4 Summary

First, feasibility of typical airfoil shape parameterization techniques was investigated through comparative studies. The reproduction of a NASA supercritical airfoil showed that the extended Joukowski airfoil was not insufficient for transonic airfoil shape designs. This study also showed that the parameterization using orthogonal shape functions is not suited for EA-based optimizations.

The aerodynamic airfoil shape optimizations ensured that the performance of the designed airfoil greatly depends on the choice of the parameterization techniques. EA using the PARSEC airfoils succeeded in finding the airfoil shape of the best performance, thanks to the selection of design

parameters based on the knowledge of transonic flow around an airfoil. Because the parameter set of the PARSEC airfoils represents important features of the given design problem, they likely to be independent of each other and thus, the present EA searched the design space efficiently.

On the other hand, design parameters of the inverse Theodorsen transformation that are chosen without knowledge of the flow physics around an airfoil provided a complex objective function landscape. Because EAs typically optimize by combining valid features of different design candidates, the performance of EAs decreases significantly for such design problems.

Then, a crossover operator based on structured coding has been proposed for EAs. The coding structure of the design variables is developed according to the epistasis analyzed by the experimental design. The present approach was applied to an aerodynamic shape design of a transonic wing where the wing shape is modeled using the parameter sets defined by the extended Joukowski airfoils and by the PARSEC airfoils. Aerodynamic optimizations of a transonic wing demonstrated that the structured coding for EAs is a promising approach to find a global optimum in practical applications. The design results also confirm that the PARSEC is an adequate technique for transonic wing shape parameterization. The improved Pareto front is obtained by EA based on the proposed structured coding using the PARSEC.

References

[1] Davidor, Y., *Genetic Algorithms and Robotics: A Heuristic Strategy for Optimization*, World Scientific, Singapore, 1991, Chap. 9.

[2] Barker, T. B., *Quality by Experimental Design*, Second edition, Marcel Dekker, Inc., New York, 1994.

[3] Jameson, A., "Optimum Aerodynamic Design via Boundary Control," *AGARD-VKI Lecture Series, Optimum Design Methods in Aerodynamics*, von Karman Inst. For Fluid Dynamics, Rhode Sait Genese, Belgium, 1994.

[4] Reuther, J. J. and Jameson, A., "A Comparison of Design Variables for Control Theory Based Airfoil Optimization," sixth International Symposium on Computational Fluid Dynamics, Lake Tahoe, Nevada, Sept. 1995.

[5] Jones, R. T., *Wing Theory*, Princeton University Press, Princeton, NJ, 1990, Chap. 3.

[6] Theodorsen, T. and Garrick, I. E. "General Potential Theory of Arbitrary Wing Sections," NACA TR 452, 1933.

[7] Obayashi, S., "Pareto Genetic Algorithm for Aerodynamic Design Using the Navier-Stokes Equations," *Genetic Algorithms and Evolution Strategy in Engineering and Computer Science*, John Wiley & Sons, Ltd, Chichester, U.K., 1998, pp.245-266.

[8] Doorly, D. J. and Peiro, J., "Supervised Parallel Genetic Algorithms in Aerodynamic Optimization," AIAA-97-1852, 1997.

[9] Chang, I., Torres, F. J. and Tung C., "Geometric Analysis of Wing Sections," NASA TM 110346, 1995.

[10] Abbott, I. and von Doenhoff, A., *Theory of Wing Sections*, Dover Publications, New York, 1949.

[11] Sobieczky, H, "Parametric Airfoils and Wings," *Recent Development of Aerodynamic Design Methodologies –Inverse Design and Optimization –*, Friedr. Vieweg & Sohn Verlagsgesellschaft mbH, Braunschweig/Wiesbaden, Germany, 1999, pp.72-74.

[12] Harris, C. D., "NASA Supercritical Airfoils," NASA TP 2969, 1990.

[13] Jameson, A. and Caughey, D. A., "A Finite Volume Method for Transonic Potential Flow Calculations," AIAA Paper 77-677, 1977.

[14] Jacobs, P. F., "Experimental Trim Drag Values and Flow-Field Measurements or a Wide-Body Transport Model with Conventional and Supercritical Wings," NASA TP 2071, 1982.